

## Swirl Effect on the Spray Characteristics of a Twin-Fluid Jet

**Byung-Joon Rho,\* Shin-Jae Kang,\* Je-Ha Oh\*\* and Sam-Goo Lee\*\***

(Received June 10, 1997)

In the liquid fuel combustion chamber, employed fuel must be atomized before being injected into the combustion zone. Therefore, the complete fuel atomization is the most important condition for the combustion efficiency. The atomization quality strongly affects the combustion performance, exhaust pollutant emissions, and flame stability. Therefore, the whole process of spray atomization is of fundamental significance. During past decades many experimental and theoretical studies in this field have been carried out and some improved results have been obtained. Two-phase atomizers, having a variety of advantages such as spray uniformity, appreciable atomization, and smaller SMD with an increase of ambient gas, are considered to be applied in various industrial processes. The purpose of present study is to investigate the mean velocity, turbulence shear stress, turbulence intensity, mean drop size distribution, and droplet data rate in a two-phase swirling jet using PDPA systems.

**Key Words:** Twin-Fluid, Swirler, Sauter Mean Diameter (SMD), Phase Doppler Particle Analyzer (PDPA), Air/Liquid Mass Flow ratio (ALR), Reynolds Stress, Hollow-Cone

### Nomenclature

*ALR* : Air to liquid mass flow ratio  
*b* : Half-width [mm]  
*d* : Diameter of the nozzle exit [mm]  
*SMD* : Sauter Mean Diameter [ $\mu\text{m}$ ]  
*U* : Axial mean velocity [m/s]  
*V* : Radial mean velocity [m/s]  
*W* : Tangential mean velocity [m/s]  
*U<sub>d10</sub>* : Axial mean velocity with droplet diameter of less than 10  $\mu\text{m}$  [m/s]  
*U<sub>cl</sub>* : Center-line axial mean velocity [m/s]  
*u'RMS* : Root mean square of axial fluctuation velocity [m/s]  
*u'v'* : Axial and radial turbulent shear stress [ $\text{m}^2/\text{s}^2$ ]  
*u'w'* : Axial and tangential turbulent

shear stress [ $\text{m}^2/\text{s}^2$ ]  
*v'w'* : Radial and tangential turbulent shear stress [ $\text{m}^2/\text{s}^2$ ]  
*X* : Coordinate of axial direction [mm]  
*Y* : Coordinate of radial direction [mm]  
 $\Phi$  : Swirl angle

### 1. Introduction

The effects of liquid fuel injection on combustor performance have been widely investigated so as to enhance the fuel economy and to reduce its exhaust emissions such as unburned-hydrocarbon. Among other things, the earth's environmental concerns have become more important than ever before. Thus, considerable attention is being concentrated on the fuel injection systems for most of the combustion engines now in use due to the ever tightening controls on environmental pollutants. For these reasons, a wide range of research works for the air-assisted injection system with swirl was carried out to satisfy the future

\* Professor, Dept. of Mechanical Engrg., Chonbuk National University, Automobile High Technology Research Institute

\*\* Graduate School, Department of Precision Mechanical Engineering, Chonbuk National University

antipollution regulations. Therefore, automotive manufacturers are focusing on combustion systems providing low levels of exhaust emissions. In some earlier works on the two-phase atomizer, Zhao et al. (1986) investigated the drop size distributions using a swirling airblast atomizer. Mao (1987) also reported that SMD and air to fuel mass flow rate ratios have linear correlation, which is valid for certain test conditions. Subsequently, Mao (1991) studied the effect of the air swirler and spray flame stability. Other workers have also reported appreciable conclusions of swirling combustion chamber on spray performance. Elkoth et al. (1978) analyzed the atomization performance in the geometrically swirling atomizer with a wide range of operating conditions. Ward and Bossard et al. (1991) made measurements using a PDPA system to examine the atomizing characteristics. They summarized that the air assist atomizer could produce hollow cone sprays having a SMD of about 20 to 25  $\mu\text{m}$ , and that atomization improved with higher ratio of air/liquid. Rho et al. (1995) made measurements on the atomization characteristics, and derived an expression that there would be an absolute correlation between SMD and ALR. Lefebvre et al. (1975, 1991) studied on the factors influencing the mean drop size. The main parameters governing the atomization are the air velocity, air/liquid ratio, surface tension, liquid viscosity, air density, and initial sheet thickness of the sprays issuing from the nozzle. Rho et al. (1994) investigated the radial spray characteristics in a plain-jet twin fluid nozzle, and concluded that SMD increases with the liquid supply and decreases with an air supply velocity. Brena de la Rosa et al. (1989) reported results of the effect of swirl on the dynamic behavior of drops and on the velocity and turbulence fields using PDPA. Rao and Lefebvre (1975, 1978) using swirl pressure atomizers have shown that increase in fuel injection pressure and air velocity tends to produce not only a reduction in mean drop size but a more uniform drop size distribution. The prerequisites for the atomization of sprays are that drop size ejecting from the nozzle should be uniform, and that constant mixing rate between

air and fuel is required. Two-phase atomizers are utilized very often to obtain better atomization. Because of its wide applications in practice, it has attracted the attention of many researchers.

This paper is being focused on the flow structures in a two-phase swirling jet, which is considered to play an important role in determining the high performance of fuel injectors. In order to achieve these goals, we have designed an air-assisted swirling injector which has conspicuously improved fuel atomization. Our specially designed air-assisted swirler atomizes the liquid fuel satisfactorily by causing the air to collide and mix, consequently, decreasing the drop diameter as a result of dispersion by its centrifugal momentum.

## 2. Experimental Apparatus

In this experiment, in order to improve the turbulence mixing characteristics between compressed-air into the combustor and liquid fuel, an air swirler was attached to the twin fluid nozzle. Figure 1 shows the nozzle geometry of swirl jet to be used in this experiment. The high velocity air impinges on the liquid, which is typical in the external mixing nozzle. Swirlers have been designed to have an angle of 0°, 22.5°, 45°, and 64.2° respectively as shown in Fig. 1.

The test facility illustrated schematically in Fig. 2 was used to make measurements.

As working fluids water and air were used, and each flow rate was controlled by a rotary compressor to reduce the surge. Continuous and

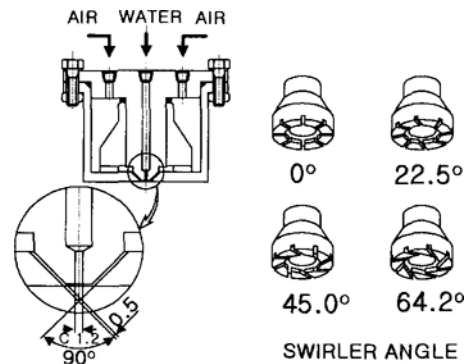


Fig. 1 Schematics illustrating the swirler nozzle.

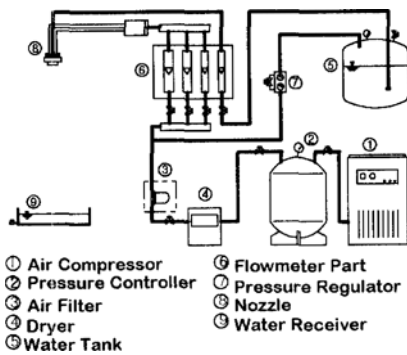


Fig. 2 Schematic diagram of test facility.

steady liquid fuel injection was generated by a pressurized fuel tank. Flow meters and pressure transducers have been carefully calibrated to obtain the exact mass flow rates. Particle diagnostics were carried out by a 3-dimensional PDPA system for a fast analysis of the global and local characteristics of a spray, which can also measure the droplet size and velocity simultaneously, consisting of a transmitter optics with a 750mW Ar-ion laser, receiver optics as a scattered light collection system using five photomultipliers, signal processor Model Dantec 58N10, and data acquisition system including a computer. Due to the measurement principle of this instrument, a Bragg cell that produces an optical frequency shift of 40MHz was used to separate the shifted and unshifted beams in the optical transmission system. The high voltage power supply of 1304V was set to carry out this experiment. At each measuring volume point, ten thousands of data sampling within 30 seconds were selected. The material used for the construction of swirlers is a Brass that could be manufactured easily and well prevented erosion. A specially designed nozzle mount and 3-dimensional automatic traversing system were installed for the measurements.

### 3. Results and Discussion

In order to see the dispersion phenomena of twin fluid swirling jet, the half-width of flow structure, plotting along the downstream of the axial distance, is illustrated in Fig. 3. It shows that the half-width of stream with increasing

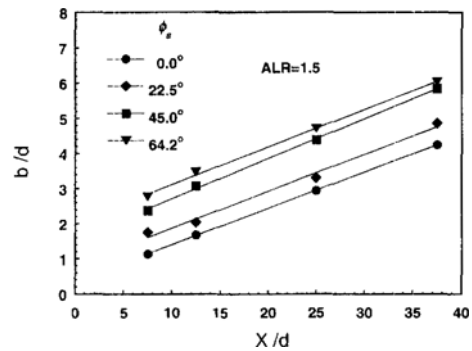


Fig. 3 Comparison of half-width with swirl angle.

swirl angle, in all cases, linearly increases and is correlated along with the axial distances. The feature is attributed to the large variation in the droplet transport according to the swirl effect, which can be presumably explained; sufficient momentum to disperse the spray behavior radially. Elucidation of this outward transport phenomenon in conjunction with both the nonswirling and swirling sprays is evident by examining the spray half-width, which has a greater sensitivity to the axial distances. The compared value of half-width increases evidently at all the axial stations, with higher swirling spray extending to much larger radial positions as compared to the lower and nonswirling cases. As an example, for  $\phi_s = 64.2^\circ$ , it increases from approximately 2.8 at  $X/d = 7$  to 6 at  $X/d = 38$ . This variation with axial position along the centerline is also clear when  $\phi_s = 0^\circ$ . Accordingly, the results indicate an increase in radial spread of the spray substantiates the radial droplet dispersion phenomena based on the centrifugal effects on droplet transport.

Non-dimensional profiles of the axial velocities illustrate similarity distributions independent of swirling angle measured at  $X/d = 15$  as shown in Figs. 4(a)-4(b), where the ALR is 1.5, 4.5, respectively. From these figures, results indicate that the magnitude of the droplet axial mean velocity decays with increasing radial position from the centerline to the spray outer regions for both the lower and higher ALR cases. The axial velocity components of the droplets for the swirling and nonswirling sprays exhibit maxima at the spray center, namely,  $Y/b = 0$ . This shows

another significant feature that axial maximum values comprise the minimum radial value on account of their own axial penetration. When compared to the lower swirling case, the values of  $\psi_s = 64.2^\circ$  for the ALR of 1.5 at the region of  $Y/b = 1.1$  to 2.0 are comparatively low. This is mainly because the centrifugal effects tend to diminish axial momentum and develop more spatial uniformity. This will be discussed more in detail in the following section. From the Fig. 4 (a), after passing  $Y/b = 2.0$ , the droplet transport indicate peculiar distributions compared to those of ALR of 4.5. It is also evident that there is an explicit similarity except for the case of  $64.2^\circ$  at ALR of 1.5. This is partly considered that in a lower ALR, droplets from the swirling nozzle are dispersed progressively to the outer regions, then, after reaching a maximum value, the velocities are abruptly decreased owing to the relatively low air velocity. Most of the higher air-mass flow rates, it appears that spray droplets issuing from the swirling nozzles are more dispersed due to the centrifugal forces.

Figures 5(a)–5(b) show the non-dimensional variation of radial velocity with different swirlers at  $X/d = 15$  from the nozzle exit. By comparing the results from the figures, it is considered that the radial mean velocity components increase with radial distances. It is also noted that the radial maximum velocity at the ALR of 1.5 is found at the region of  $Y/b = 1$ , and then decreases gradually. For the higher ALR of 4.5, on the other hand, velocity components by degrees increases along the distances, then, after reaching

a maximum value at about  $Y/b = 1.3$ , decreases progressively as a result of relatively higher dispersion phenomenon. Thus, it is again interesting to recognize that in the case of  $\psi_s = 64.2^\circ$  for both the lower and higher ALRs, the value of radial mean velocity is the largest nearly at the  $Y/b = 1$  for the swirling angle of  $\psi_s = 64.2^\circ$  but is much significantly the smallest for the ALR of 4.5 case. This difference between two cases may be attributed to the presence of relatively strong air in the latter case that promotes the axial momentum to penetrate further than that of radial dispersion. That is, air velocity for the higher ALR is one of the key parameters affecting the spray behavior most. In contrast, the swirling angles are the dominant factors influencing the droplet transport for the lower case of ALR. The profiles of radial mean velocity show that it starts from the reasonable value of zero at the spray center of  $Y/b = 0$  for both cases. On the ground that the peak values of axial mean velocity exist at the spray center (as shown in Figs. 4(a)–4(b)), these data indicated in Figs. 5(a)–5(b) are worth considering the fact that axial strong penetration of droplet transport means radial weak distribution. As it can be seen from Figs. 4(a)–4(b), for  $\psi_s = 64.2^\circ$  in the case of ALR = 1.5, assuming that the droplet velocities are almost the same for the other cases, the values of velocity having much smaller when compared to those of others are more crucial clues to obtain an acceptable reason why the values for the swirl angle  $\psi_s = 64.2^\circ$  are so high as shown in Fig. 5(a). As discussed before, it is because the outward centrifugal effects with

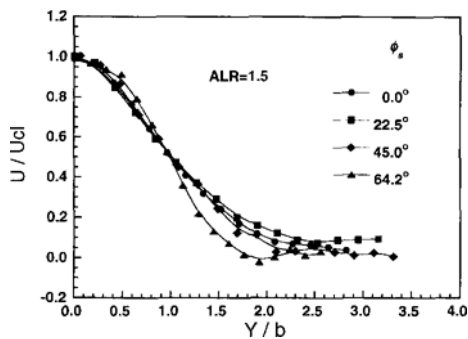


Fig. 4(a) Profiles of axial mean velocity with different swirl angles and ALRs.

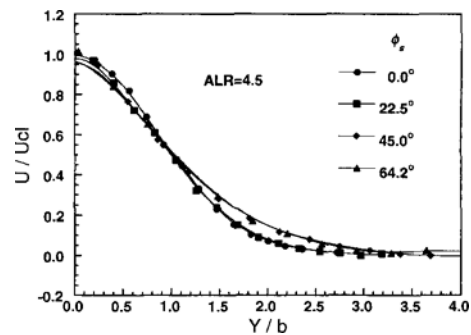


Fig. 4(b) Profiles of axial mean velocity with different swirl angles and ALRs.

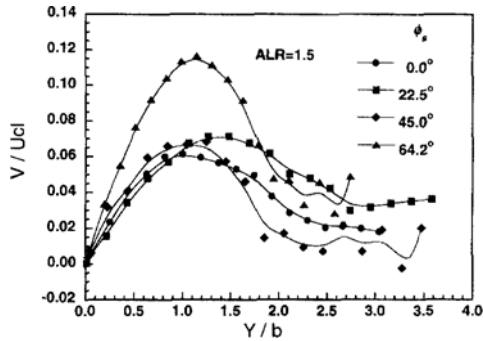


Fig. 5(a) Profiles of radial mean velocity with different swirl angles and ALRs.

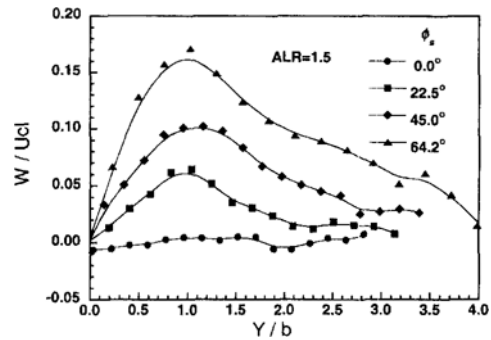


Fig. 6(a) Profiles of tangential mean velocity with different swirl angles and ALRs.

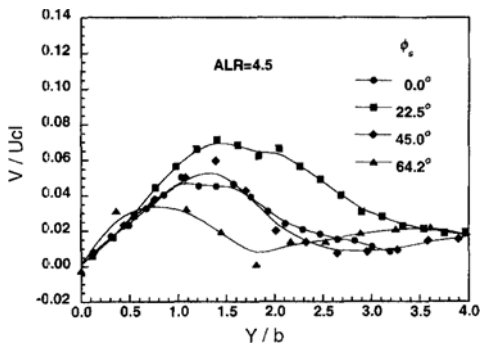


Fig. 5(b) Profiles of radial mean velocity with different swirl angles and ALRs.

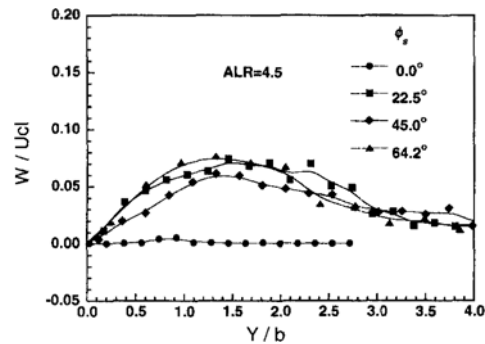


Fig. 6(b) Profiles of tangential mean velocity with different swirl angles and ALRs.

strong swirl are impeding the axial momentum, or its own inertia force to go further downstream and eventually enhance the droplet transport more spatially uniform and disperse it toward the radial direction. Therefore, this result suggests that the presence of the even minimal axial velocity difference seems to be meaningful because the droplet deceleration in the axial direction in a sense means wider dispersion in the radial transport. After the region of  $Y/b=2.0$ , there would exist axially divergent stations (Fig. 4(a)), and convergent regions (Fig. 4(b)). The former can be easily confirmed by examining Fig. 5(a), the latter by Fig. 5(b). To summarize, axial divergence means more unstable or volatile to spread radially, and axial convergence means radially stable or nearly constant.

It was also of interest to examine the effects of tangential velocity on the ALR and swirler angle. Figures 6(a)–6(b) show a normalized tangential velocity distributions. As shown in Fig. 6(a), the

tangential velocity components increase with the swirling angles in case of  $ALR=1.5$ , while this increasing trend depending upon the swirling angle almost disappeared at  $ALR=4.5$  as shown in Fig. 6b. Another interesting characteristic is that there isn't any explicit change of tangential velocity for the nonswirling spray regardless of its own ALR. It is convinced from the results that the effect of the swirler angle on the tangential velocity distribution works only for the lower case of ALR.

In general, since the atomization process occurs as a result of interaction between a liquid and the ambient air, detailed measurements have been carried out for a fixed ALR of 1.5 to compare the mean velocity components of air and droplets (less than  $10 \mu\text{m}$ ) as illustrated in Fig. 7. In the radial direction, for the swirler angle of  $0^\circ$  (see Fig. 7(a)), the results at most of the sampling locations show that all the air velocity distributions are explicitly smaller than those of droplets both in

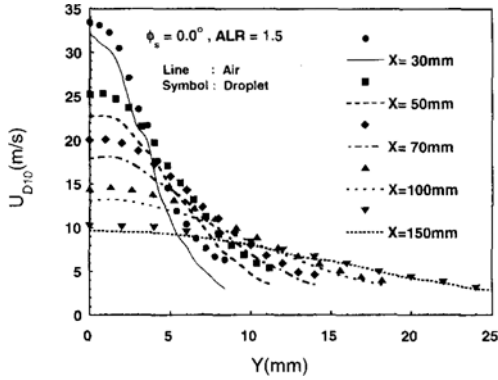


Fig. 7(a) Compared axial velocity variation between air and droplet (diameter of less than 10  $\mu$  m).

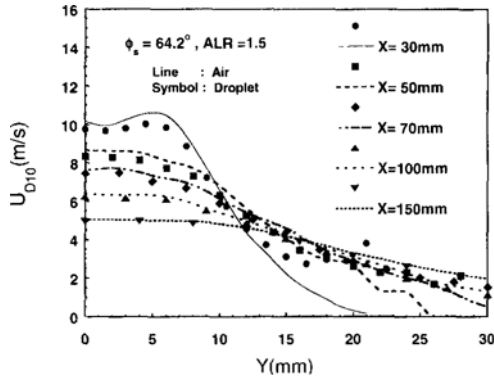


Fig. 7(b) Compared axial velocity variation between air and droplet (diameter of less than 10  $\mu$  m).

the center and outer regions. On the other hand, Fig. 7(b) exhibits interesting features which appear to be characteristic for a wider swirling angle. The droplet axial mean velocity near the center region tends to be lower than the air. In the outer region, however, the droplet velocity decreases gradually. These trends are typical when varying the swirler angle. This is definitely attributed to the centrifuge effect in the swirl regions with a relative momentum of the liquid jet and the swirling air.

For the analysis of turbulent mixing in the flow field, the non-dimensional variations of Reynolds stress profiles of droplets are shown in Fig. 8. As illustrated clearly in Figs. 8(a) and 8(b), the Reynolds stresses of  $u'v'$  and  $v'w'$  are developed more highly with the increasing swirler angle.

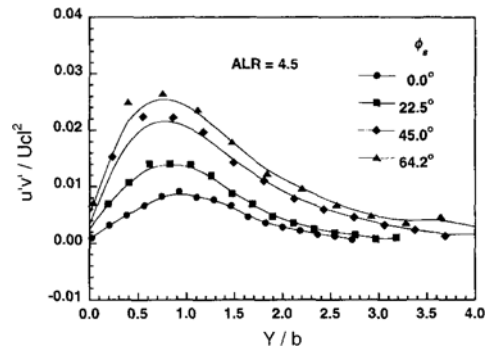


Fig. 8(a) Profiles of Reynolds stress.

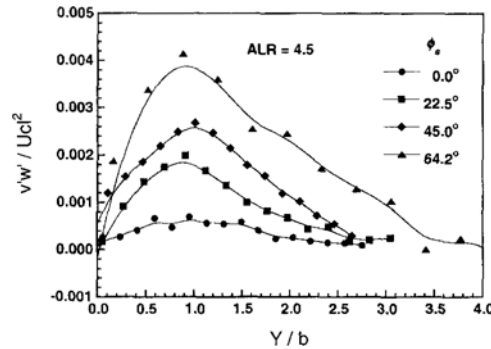


Fig. 8(b) Profiles of Reynolds stress.

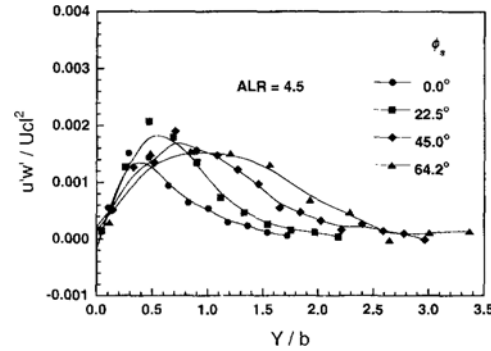


Fig. 8(c) Profiles of Reynolds stress.

This phenomenon is quite remarkable and can be possibly substantiated by the assumption that the turbulent mixing trends in the flowfield are prominently affected with an increment of swirl. On the other hand, the components of  $u'w'$  (see 8(c)) shows a similar maximum values but distributions are not so explicitly distinctive. The RMS profiles at a fixed ALR of 4.5 are shown in Fig. 9. Due to the dispersion momentum, relatively higher values of fluctuating components have been obtained

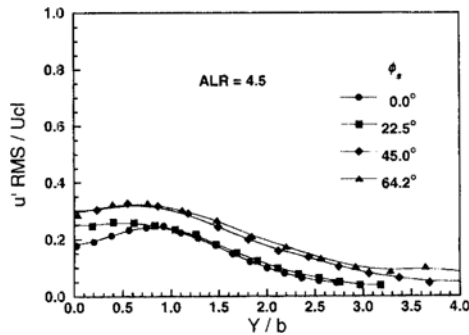


Fig. 9 Variation of turbulence intensity along the axis.

for  $\phi_s = 64.2^\circ$  and the difference is about more than 50%, which is coincident with figures 3 and 10. Through the experimental results, RMS values were found to be higher for the smaller droplets with higher air supply pressures, namely, higher ALR.

Figure 10 illustrates the variations of mean drop size measured at the centerline axial downstream distances with swirl angle for a constant ALR of 5.5. The SMD is defined as  $\sum N_i D_i^3 / \sum N_i D_i^2$  where,  $N_i$  is the number of drops in size range  $i$ , and  $D_i$  is the middle diameter of size range  $i$ . Therefore, SMD is the diameter of the drop whose ratio of volume to surface area is the same as that of the entire spray. In relatively lower swirler angles, the droplet diameters in the vicinity of the atomizer exit definitely increase, then, after reaching a maximum drop size, the SMD structure shows a gradual decrease to the extent that it reaches its minimum value, and gradually changed again owing to the presumably coalescence effect along with axial distances. Meanwhile the results obtained for swirler angle of  $64.2^\circ$  show quite a few different shape; viewing the diminutive droplet diameter in upstream region of the nozzle tip is not available. This interesting feature clearly demonstrates that the probable penetration length of the liquid core and breakup region from the atomizer in a smaller swirl angles of  $0^\circ$ ,  $22.5^\circ$ , and  $45^\circ$  are comparatively long. Hence, the larger swirl angle, the shorter breakup length. This means that an increase in swirl angle raises the dispersion rate because of its own centrifugal force, and illustrates the benefi-

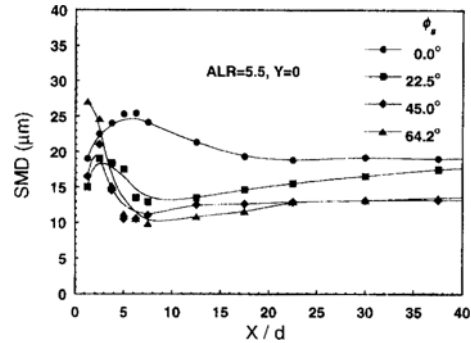


Fig. 10 Variation of drop size with swirl angle for a constant ALR of 5.5.

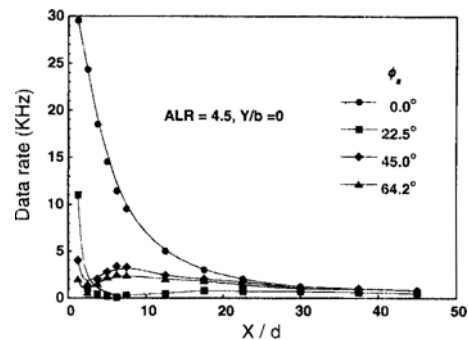


Fig. 11 Distribution of data rate along the axial direction.

cial effect of an increase in swirl angle when reducing SMD. For example (see Fig. 10), the effects of swirl on droplet diameter are emphasized by comparing the spray in the flowfield under higher swirling conditions of  $\phi_s = 64.2^\circ$  to the nonswirling case. The magnitude in Sauter mean diameter for  $\phi_s = 0^\circ$  and  $\phi_s = 64.2^\circ$  at axial locations  $X/d = 23$  and  $38$  downstream of the nozzle exit is an order of approximately  $19 \mu\text{m}$ ,  $12.5 \mu\text{m}$ ,  $19 \mu\text{m}$  and  $13.5 \mu\text{m}$ , respectively. These values in Sauter mean diameter at each axial downstream position appear to match the ones in spray half-width (see Fig. 3). This result indicates that swirl effect promotes 43%-52% decrease in SMD compared to the nonswirling condition. The profiles of Sauter mean diameter also indicate the expected reduction of spray drop diameter with increasing swirl, which is predictable as discussed in Fig. 3. It is considered that swirl, resulting in wider spray half-width, increases the radial dispersion due to the droplet centrifugal momentum. To consider

the droplet concentration in both dense and dilute phase regions. Fig. 11 shows the measured data rate. From the configuration, it definitely shows that the drop rates are inversely proportional to the distance in the lower swirler angles, compared with those of higher cases. This is mainly because there is a hollow-cone shape region along the centerline downstream arisen from the strong swirling air-stream. It is considered that at this part, droplet concentrations are relatively dilute.

#### 4. Conclusions

From the analysis of swirl effect on droplet transport, some concluding remarks can be summarized as following.

The effect of swirl is apparent by comparing the spray half-width, droplet size and turbulence intensity for all the cases. In the case of the largest swirl, the highest values are expected in spray half-width because of the centrifugal momentum, which results in the considerable increases in turbulence intensity of more than 50%, and SMD reduction of nearly 43%-52% compared to those of nonswirling spray are the characteristic feature of swirl influence. Therefore, with the larger swirl, the higher radial dispersion phenomenon due to its centrifugal momentum tends to reduce the SMD, and eventually leads to the beneficial influence to facilitate the atomization. Hence, of all the various parameters influencing the droplet distribution and atomization, it is no doubt that air velocity and optimum swirl are the most important factors.

#### References

- Brena de la Rosa, A., Bachalo, W. D., and Rudoff, R. C., 1989, "Spray Characterization and turbulence Properties in an Isothermal Spray with Swirl," ASME paper No. 89-GT-273, *34th ASME International Gas Turbine & Aeroengine Congress, Toronto, Canada, June*
- Elkotp, M. M., Rafat, N. M., Hanna, M. A., 1978, "The Influence of Swirl Atomizer geometry on the Atomization Performance," *ICLASS*, pp. 109~115.
- Lefebvre, A. H., 1991, "Twin-Fluid Atomization: Factors Influencing Mean Drop Size," *ICLASS-'91*, pp. 49~64
- Mao, C. P., 1987, "Drop size Distribution and Air Velocity Measurements in Air Assist Swirl Atomizer Sprays," *ASME*, Vol. 109, pp. 64~69
- Mao, C. P., 1991, "Effect of Air Swirlers Atomizations and Spray Flames Stability," *ICLASS-'91*, pp. 513~520
- Rho, B. J., Kang, S. J. and Choi, J. C., 1994, "A Study on the Radial Spray Performance of a Plain Jet Twin Fluid Nozzle," *Transactions of KSME*, Vol. 18, No. 3, pp. 662~669
- Rho, B. J., Kang, S. J. and Oh, J. H., 1995, "An Experimental Study on the Atomization Characteristics of a Two-Phase Turbulent Jet of Liquid Sheet Type Co-Axial Nozzle," *Transactions of KSME*, Vol. 19, No. 6, pp. 1529~1538
- Rizkalla, A. A. and Lefebvre, A. H., 1975, "The Influence of Air and Liquid Properties on Airblast Atomization," *ASME*
- Rao, K. V. L. and Lefebvre, A. H., 1975, "Fuel Atomization in a flowing Airstream," *AIAA journal*, Vol. 13, Oct. pp. 1413~1415
- Rao, K. V. L., 1978, "Liquid Nitrogen Cooled Sampling Probe for the Measurement of Spray Drop size Distribution in Moving Liquid-Air Sprays," *proceedings of the 1st ICLASS meeting*, pp. 293~300
- Ward, M. J., Bossard, J. A., Peck, R. E. and Hirleman, E. D., 1991, "Spray Characterization in Axisymmetric Swirling Combustor Flows," *ICLASS-'91*, pp. 529~537
- Zhao, Y. H., Hou, M. H. and Chin, J. S. 1986 "Drop size Distribution from Swirling Airblast Atomizers," *Atomization and Spray Technology*, pp. 3~15